Amyloid Formation

DOI: 10.1002/anie.201407323

Conformational Flexibility Tunes the Propensity of Transthyretin to Form Fibrils Through Non-Native Intermediate States**

*Jitendra K. Das, Shyam S. Mall, Aritra Bej, and Sujoy Mukherjee**

Dedicated to Professor Siddhartha Roy on the occasion of his 60th birthday

Abstract: *The formation of partially unfolded intermediates through conformational excursions out of the native state is the starting point of many diseases involving protein aggregation. Therapeutic strategies often aim to stabilize the native structure and prevent the formation of intermediates that are also cytotoxic in vivo. However, their transient nature and low population makes it difficult to characterize these intermediates. We have probed the backbone dynamics of transthyretin (TTR) over an extended timescale by using NMR spectroscopy and MD simulations. The location and extent of these motions indicates that the backbone flexibility of TTR is a cause of dissociation and destabilization, both of which are responsible for fibril formation. Importantly, approximately 10 % of wild-type TTR exists in an intermediate state, which increased to up to 28 % for pathogenic TTR mutants, for which the formation of the intermediate state is shown to be energetically more favorable compared to the wild type. This result suggests an important role for the intermediates in TTR amyloidosis.*

The conversion of native proteins into amyloid fibrils is the hallmark of a large number of protein aggregation diseases. It has been shown that this conversion is mediated by transient intermediates, the formation of which is facilitated by conformational excursions out of the native state.[1] In addition to being precursors to mature fibrils, these intermediates are increasingly believed to be primarily responsible for cytotoxicity.[2] In general, intermediate states of proteins are known to mediate various biologically important processes,[3] thus making it crucial to understand them at a molecular level. Given their transient nature and low population, these intermediates are difficult to characterize by most biophysical methods. In this work, we probed the backbone dynamics of wild-type transthyretin (WTTR) along with its clinically important mutants (L55P, V30M, V122I and T119M) and quantified their intermediate states to show a direct correlation between the formation of non-native intermediates and pathogenicity.

WTTR has been implicated in senile systemic amyloidosis owing to its deposition as amyloid fibrils in the heart, which causes cardiomyopathy. A large number of mutant forms of TTR (MTTRs) are responsible for leptomeningeal, cardiac, and neuropathic forms of familial amyloidosis.[4] The transformation of soluble TTR into amyloid fibrils is believed to follow a downhill polymerization mechanism,[4] in which TTR dissociation exposes partially unfolded monomers that can aggregate into amyloid fibrils (Figure 1). More significantly, non-native conformers of TTR have been shown to be cytotoxic in vivo,[5] which makes them biologically important targets for investigation. The crystal structures for a large number of stabilizing and destabilizing mutants have been solved over the years and found to be strikingly similar to that of WTTR,[6] thus suggesting that gross structural differences cannot explain the wide phenotypic variations between MTTRs. Although protein dynamics have been shown to be key to the misfolding of many proteins,[1] this has not been explicitly studied before with the TTR tetramer and its mutants on a residue-specific basis.

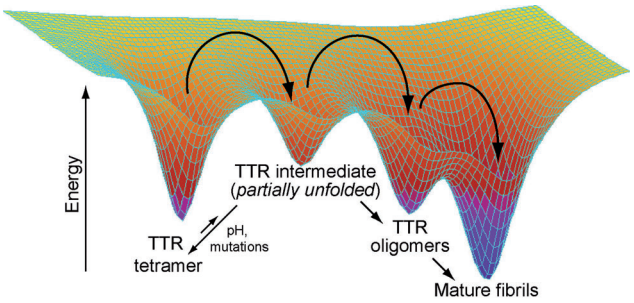

Figure 1. A free-energy landscape depicting the prominent conformational states of TTR. Arrows between energy wells denote conformational excursions of TTR from one state to another.

^{15}N relaxation rates (R_1 and R_2) and NOE are shaped by fast motions on the picosecond–nanosecond timescale. Fitting relaxation rates[7] to various motional models[8] enables the estimation of rotational diffusion tensor and order parame-

[*] J. K. Das, S. S. Mall, A. Bej, Dr. S. Mukherjee
Structural Biology and Bioinformatics division
CSIR—Indian Institute of Chemical Biology
4 Raja S. C. Mullick Road, Kolkata, West Bengal, 700032 (India)
E-mail: sujoy@csiriicb.in
mukherjee.lab@gmail.com
Homepage: https://sites.google.com/site/mukherjeelab/

[**] We thank Prof. David Wemmer for the gift of plasmids, Prof. Lewis E. Kay for programs for data fitting and critical review of the manuscript, Prof. Ad Bax for NMR pulse programs, Prof. Siddhartha Roy and Prof. Gautam Basu for stimulating discussions, the NMR facility at TIFR for 800 MHz NMR time, CSIR-4Pi for access to the supercomputing facility, Baptala Sai for help with sample preparation and T. Muruganandan for AFM microscopy. Research fellowships are acknowledged from CSIR (to J.K.D.), ICMR (to S.S.M.), and DST (to A.B. and S.M.). This work is supported by funding from CSIR.

Supporting information for this article is available on the WWW under http://dx.doi.org/10.1002/anie.201407323.

ters (S^2) that are quantitative reporters of protein dynamics.[9] For WTTR at pH 5.75, the relaxation data (Table S1 in the Supporting Information) could be best fit to an axially symmetric diffusion tensor ($D_{\parallel/\perp} \approx 1.1$) with rotational correlation time ($\tau_m \approx 21.5$ ns) consistent with a tetramer at 40 °C (Tables S2 and S11). The average S^2 for all residues was approximately 0.86, thus indicating that the WTTR backbone is fairly rigid. However, the variation in S^2 with protein sequence shows that most of the conformational flexibility was restricted to three regions (Figure 2A, red dashed lines) encompassing residues A37–W41, G57–T60, and S100–G101 which primarily include solvent-exposed residues. Not surprisingly, residues within the β-sheets appear comparatively rigid with little sign of flexibility on picosecond–nanosecond timescale (Figure 2B–D).

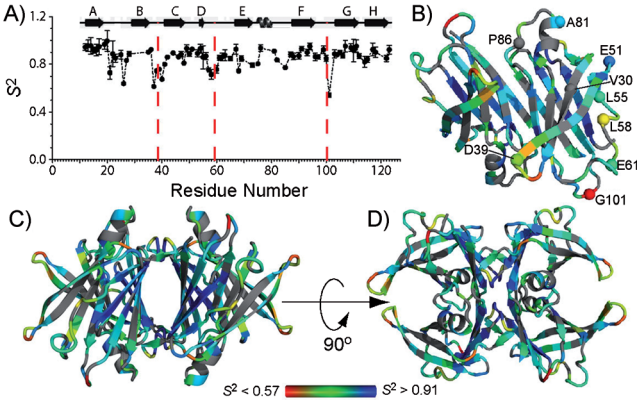

Figure 2. A) A plot of backbone ^{15}N S^2 values against WTTR sequence (from Table S2). The wire diagram depicts the secondary structure as shown in Figure S1 in the Supporting Information. B) S^2 values are mapped on the crystal structure (dimer) with the most rigid and most dynamic residues depicted in blue and red, respectively. C, D) Tetramers are assembled from the dimer (B). Residues where S^2 could not be obtained, including unassigned resonances, are shown in gray.

In addition to these fast motions, WTTR (pH 5.75) could exhibit slower dynamics in the microsecond–millisecond region (Figure 3A). This was verified by using relaxation dispersion NMR on backbone ^{15}N spins.[10] R_{ex} values were extracted from dispersion trajectories (Figure 3B and Figure S3 in the Supporting Information) and the residue-specific plot of R_{ex} shows that WTTR undergoes slow conformational fluctuations at two regions encompassing L12–S23 and R103–N124, although minor conformational flexibility is also present in the L55–H56 and F87–V93 regions (Figure 3C). R_{ex} values mapped onto the crystal structure[11] of WTTR (Figure 3C,D) show that higher conformational flexibility is almost exclusively located in the AGH β sheet, which forms the hydrophobic core of the tetramer. WTTR is overwhelmingly (> 95 %) tetrameric at submicromolar (ca. 0.72 μM) concentrations,[12] thus suggesting negligible dissociation at the concentrations (ca. mM) used for NMR studies. In the absence of dissociation, high R_{ex} values for contiguous residues in the β sheet could be attributed to a conformational exchange of each undissociated monomer from the native state (N) to a non-native intermediate state (I). A significant

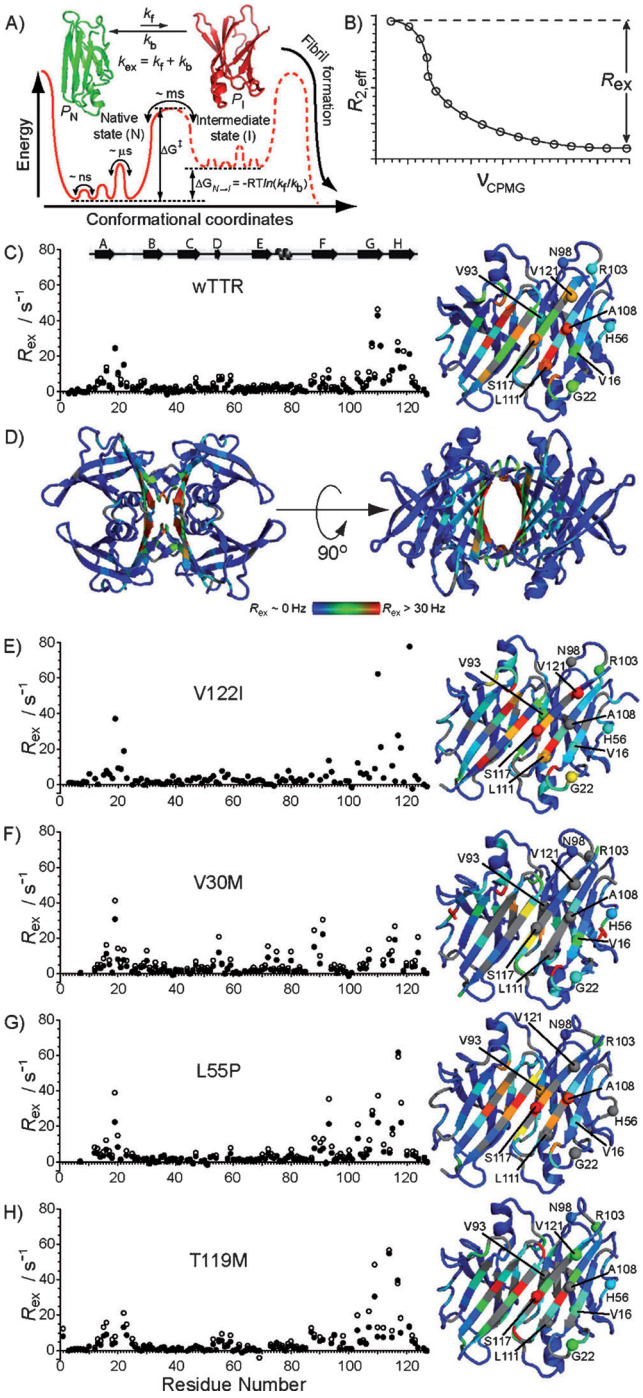

Figure 3. A) An energy diagram showing the conformational states of TTR. The bold and dashed wells denote the observable and invisible states of TTR, respectively. B) Representation of a plot of $R_{2,eff}$ against ν_{CPMG}, depicting the R_{ex} value for a typical residue. Plots of the R_{ex} values from ^{15}N relaxation dispersion experiments on WTTR (C),[11] V122I (E),[13] V30M (F),[14] L55P (G),[15] and T119M (H)[16] TTR are shown for 14.1 T (solid circles) and 18.78 T (empty circles) magnetic fields (see Table S12). R_{ex} values from the 14.1 T field were mapped onto the dimer of the respective crystal structures, with rigid residues shown in blue ($R_{ex} \approx 0$ Hz) and dynamic ones in red ($R_{ex} > 30$ Hz). The wire diagram (C) depicts secondary structure as shown in Figure S1. D) WTTR tetramers formed from the dimer (C) are shown. Residues for which R_{ex} could not be obtained are shown in gray.

lowering of TTR concentration would enable the dissociation of these non-native monomers and allow their rearrangement to form fibrils. It is also important to note that β strand H and residues in the AB and GH loops are involved in dimer and tetramer formation, respectively, thus suggesting that extensive conformational flexibility in these regions could be responsible for TTR dissociation under physiological concentrations.

The dynamic residues in WTTR were best fit to a 2-state exchange model to obtain the exchange rate ($k_{ex} = 382 \pm 7$ Hz), population of the intermediate ($P_I = 9.6 \pm 0.1\,\%$), and free energy difference between the conformers ($\Delta G_{N\rightarrow I} = 1.39 \pm 0.02$ kcal mol^{-1}, Table 1). To verify that the formation of the non-native state is linked to fibril-forming propensity, we probed the backbone dynamics of clinically important MTTRs. The results of fast-timescale dynamics in MTTRs are essentially similar to those for WTTR, with minor differences in the flexibility of the DE loop region (Tables S3–S8, S11 and Figure S2B–D). However, the MTTRs displayed varied extents of motion on the millisecond timescale, even though the dynamic regions were similar (Figure 3 E–G). V30M and L55P TTRs were not stable at pH 5.75, but at pH 7 they showed an appreciably higher population of intermediates ($P_I \approx 27.9$ and 16.2 %), faster kinetics of conversion ($k_f \approx 118$ and 95 Hz), and a lower free-energy difference ($\Delta G_{N\rightarrow I} \approx 0.59$ and 1.02 kcal mol^{-1}) with respect to WTTR at pH 5.75 (Table 1). These results suggest that pathogenic MTTRs at pH 7 form more intermediates than WTTR at pH 5.75.

T119M is a stabilizing mutation that can prevent V30M TTR from aggregating in vivo by stabilizing tetramer-forming contacts.[17] However, it is not known whether T119M TTR is conformationally flexible and forms fibrils readily upon dissociation. NMR studies with T119M TTR show it to be appreciably dynamic although its k_f and P_I values are much lower than those of the pathogenic mutants (Table 1). The presence of conformational flexibility is not surprising per se and indicates that T119M TTR could form fibrils as long as the tetramers are sufficiently dissociated. We found that WTTR forms high-quality fibrils at pH 5.2 or less but T119M TTR fibrils are formed at pH 3.6 (and not at pH 5.2; Figure S8).

Table 1: Summary of the kinetic and thermodynamic parameters of TTR proteins.[a]

TTR variant	k_{ex} [Hz][b]	P_I [%]	k_f [Hz]	ΔG^{+}[c] [kcal mol^{-1}]	$\Delta G_{N\rightarrow I}$[d] [kcal mol^{-1}]
WTTR	382 ± 7	9.6 ± 0.1	37 ± 1	16.1 ± 0.01	1.39 ± 0.02
V30M[e]	421 ± 11	27.9 ± 5.1	118 ± 31	15.3 ± 0.16	0.59 ± 0.17
L55P[e]	585 ± 8	16.2 ± 0.5	95 ± 4	15.46 ± 0.03	1.02 ± 0.03
T119M	618 ± 10	11.9 ± 0.2	74 ± 2	15.62 ± 0.02	1.24 ± 0.02

[a] Dynamic parameters could not be extracted owing to excessive line broadening with V122I TTR. [b] Exchange rate (k_{ex}) = forward rate (k_f) + backward rate (k_b). [c] ΔG^{+} is the activation energy for native state (N) as in Figure 3 A. [d] The free-energy difference between the native and intermediate (I) states, $\Delta G_{N\rightarrow I} = G_I - G_N$. [e] Experiments were performed at pH 7.

The EF loop–helix region,[18] along with β strands C and D,[19,20] is believed to play a crucial role in TTR destabilization. However, S^2 values could not be obtained for many residues in these regions. ^{1}H/^{2}H exchange studies with soluble TTR[19] and EPR studies on fibrils[20] have suggested the destabilization of the CBEF β sheet (see Figure S1) to be important for the aggregation of TTR; the authors of the latter study added that their observations could also be explained by a destabilization of the DAGH sheet. Our experiments showed significant mobility of the DAGH sheet but only intermittent motion in the CBEF sheet, similar to that observed for monomeric mutants of TTR.[21] Recent solid-state NMR data on WTTR fibrils, however, suggest a more significant rearrangement of native structure than previously thought, with strands D, G, and H forming the amyloid core.[22] To gain atomistic insight into the extent of the conformational flexibility, we performed molecular dynamics (MD) simulations and found extensive motion in four regions of all TTR proteins (Figure S10), a result consistent with our NMR studies on the picosecond–nanosecond timescale. All of the proteins exhibited conformational flexibility in their C and D β-strand/loop residues, which increased their distance from the adjacent β strands B and A, respectively. We looked at various parameters that report on the perturbation of the native structures and are relevant to fibril formation.[19,23] These include mean distances between strands A and D and strands B and C, backbone RMSD, SASA, and number of protected hydrogen bonds. In all cases (Table 2), we found that pathogenic V30M and L55P TTRs exhibit more perturbation from ground-state structures than WTTR or T119M TTR and that the magnitudes of these perturbations are proportional to reported instabilities of these variants.[24]

Table 2: Results of 1 μs all-atom MD simulations on TTR proteins.

TTR variant	Mean distance A–D, B–C [Å][a]	Backbone RMSD [Å][b]	SASA [nm^2][c]	Mean H bonds[d]	$\Delta G^{[e]}$ [kcal mol^{-1}]
WTTR	9.85	2.40	51.89	359	3.4 ± 0.5
V122I	9.41	2.05	52.59	356	–
V30M	10.05	2.59	52.02	352	2.9 ± 0.4
L55P	11.51	2.77	53.07	340	2.5 ± 0.5
T119M	9.56	2.30	51.56	365	5.8 ± 0.4

[a] The distances between two strands were calculated from the distances between their centers of mass. The mean distances between strands A and D and strands B and C are reported. [b] RMSD = root mean square deviation of the backbone heavy atoms. [c] SASA = solvent accessible surface area. [d] The average number of intramolecular hydrogen bonds (excluding solvent). [e] From a previous report.[24]

In summary, we found that the most prevalent TTR proteins exist in conformational exchange with a non-native intermediate, the transient nature of which had prevent their biophysical characterization. We show that in comparison to wild-type TTR, the intermediates of disease-causing mutants have higher populations, lower free energies, and faster kinetics of conversion from their native states, all of which facilitate the aggregation of TTR. Our study establishes

a direct correlation between the conformational flexibility of TTR and its known amyloidogenic propensity, thereby opening the possibility of using protein dynamics as a predictor of pathogenicity for TTR and possibly in other diseases involving protein aggregation. Finally, a better understanding of the aggregation process is also likely to help in the development of molecules to stabilize TTR structure, neutralize toxic oligomers, or inhibit fibril formation, as has been possible for TTR[25] and in other systems.[26,27]

Received: July 17, 2014
Revised: August 29, 2014
Published online: September 22, 2014

Keywords: Amyloids · misfolding intermediates · NMR spectroscopy · protein folding · transthyretin

[1] F. Chiti, C. M. Dobson, *Nat. Chem. Biol.* **2009**, *5*, 15.
[2] C. Cecchi, M. Stefani, *Biophys. Chem.* **2013**, *182*, 30.
[3] A. J. Baldwin, L. E. Kay, *Nat. Chem. Biol.* **2009**, *5*, 808.
[4] S. M. Johnson, S. Connelly, C. Fearns, E. T. Powers, J. W. Kelly, *J. Mol. Biol.* **2012**, *421*, 185.
[5] N. Reixach, S. Deechongkit, X. Jiang, J. W. Kelly, J. N. Buxbaum, *Proc. Natl. Acad. Sci. USA* **2004**, *101*, 2817.
[6] A. Hörnberg, T. Eneqvist, A. Olofsson, E. Lundgren, A. E. Sauer-Eriksson, *J. Mol. Biol.* **2000**, *302*, 649.
[7] N. A. Lakomek, J. Ying, A. Bax, *J. Biomol. NMR* **2012**, *53*, 209.
[8] A. M. Mandel, M. Akke, A. G. Palmer, *J. Mol. Biol.* **1995**, *246*, 144.
[9] G. Lipari, A. Szabo, *J. Am. Chem. Soc.* **1982**, *104*, 4546.
[10] P. Vallurupalli, D. F. Hansen, E. Stollar, E. Meirovitch, L. E. Kay, *Proc. Natl. Acad. Sci. USA* **2007**, *104*, 18473.
[11] T. Klabunde, H. M. Petrassi, V. B. Oza, P. Raman, J. W. Kelly, J. C. Sacchettini, *Nat. Struct. Mol. Biol.* **2000**, *7*, 312.
[12] A. R. Hurshman Babbes, E. T. Powers, J. W. Kelly, *Biochemistry* **2008**, *47*, 6969.
[13] A. M. Damas, S. Ribeiro, V. S. Lamzin, J. A. Palha, M. J. Saraiva, *Acta Crystallogr. Sect. D* **1996**, *52*, 966.
[14] D. B. B. Trivella, L. Bleicher, L. d. C. Palmieri, H. J. Wiggers, C. A. Montanari, J. W. Kelly, L. M. T. R. Lima, D. Foguel, I. Polikarpov, *J. Struct. Biol.* **2010**, *170*, 522.
[15] L. Cendron, A. Trovato, F. Seno, C. Folli, B. Alfieri, G. Zanotti, R. Berni, *J. Biol. Chem.* **2009**, *284*, 25832.
[16] M. P. Sebastião, V. Lamzin, M. J. Saraiva, A. M. Damas, *J. Mol. Biol.* **2001**, *306*, 733.
[17] P. Hammarstrom, F. Schneider, J. W. Kelly, *Science* **2001**, *293*, 2459.
[18] S. K. Palaninathan, N. N. Mohamedmohaideen, W. C. Snee, J. W. Kelly, J. C. Sacchettini, *J. Mol. Biol.* **2008**, *382*, 1157.
[19] K. Liu, H. S. Cho, H. A. Lashuel, J. W. Kelly, D. E. Wemmer, *Nat. Struct. Mol. Biol.* **2000**, *7*, 754.
[20] A. A. Serag, C. Altenbach, M. Gingery, W. L. Hubbell, T. O. Yeates, *Nat. Struct. Biol.* **2002**, *9*, 734.
[21] K. H. Lim, H. J. Dyson, J. W. Kelly, P. E. Wright, *J. Mol. Biol.* **2013**, *425*, 977.
[22] D. A. Bateman, R. Tycko, R. B. Wickner, *Biophys. J.* **2011**, *101*, 2485.
[23] E. J. Nettleton, M. Sunde, Z. Lai, J. W. Kelly, C. M. Dobson, C. V. Robinson, *J. Mol. Biol.* **1998**, *281*, 553.
[24] A. Quintas, D. C. Vaz, I. Cardoso, M. J. M. Saraiva, R. M. M. Brito, *J. Biol. Chem.* **2001**, *276*, 27207.
[25] C. E. Bulawa, S. Connelly, M. Devit, L. Wang, C. Weigel, J. A. Fleming, J. Packman, E. T. Powers, R. L. Wiseman, T. R. Foss, I. A. Wilson, J. W. Kelly, R. Labaudiniere, *Proc. Natl. Acad. Sci. USA* **2012**, *109*, 9629.
[26] P. Arosio, M. Vendruscolo, C. M. Dobson, T. P. Knowles, *Trends Pharmacol. Sci.* **2014**, *35*, 127.
[27] A. Aguzzi, T. O'Connor, *Nat. Rev. Drug Discovery* **2010**, *9*, 237.

